Draft Version 3.0: June 29, 2010

The GlueX Experiment in Hall-D

The GlueX Collaboration*

The goal of the GlueX experiment is to provide critical data needed to address one of the outstanding and fundamental challenges in physics – the quantitative understanding of the confinement of quarks and gluons in quantum chromodynamics (QCD). Confinement is a unique property of QCD and understanding confinement requires an understanding of the soft gluonic field responsible for binding quarks in hadrons. Hybrid mesons, and in particular exotic hybrid mesons, provide the ideal laboratory for testing QCD in the confinement regime since these mesons explicitly manifest the gluonic degrees of freedom. Photoproduction is expected to be particularly effective in producing exotic hybrids but there is little data on the photoproduction of light mesons. GlueX will use the coherent bremsstrahlung technique to produce a linearly polarized photon beam. A solenoid-based hermetic detector will be used to collect data on meson production and decays with statistics after the first full year of running that will exceed the current photoproduction data in hand by several orders of magnitude. These data will also be used to study the spectrum of conventional mesons, including the poorly understood excited vector mesons. In order to reach the ideal photon energy of 9 GeV for this mapping of the exotic spectrum, 12 GeV electrons are required. This document updates the physics goals, the beam and apparatus of the GlueX detector in Hall-D since the original proposal was presented to PAC 30 in 2006 [1].

I. INTRODUCTION

Quantum chromodynamics (QCD) provides a clear description of the strong interaction of quarks and gluons at high energy; however, obtaining quantitative predictions from QCD at low energy remains challenging. Interestingly, it is at these low energies that we observe the most obvious physical manifestation of QCD, the spectrum of particles that make up the universe we live in, baryons and mesons. While models do provide predictions for this spectrum, to obtain this spectrum as a solution to QCD is currently only possible using numerical techniques to calculate it, lattice QCD.

The observation, nearly five decades ago, that mesons are grouped in nonets, each characterized by unique values of J^{PC} spin (J), parity (P) and charge conjugation (C) quantum numbers led to the development of the quark model. Within this picture, mesons are bound states of a quark (q) and antiquark ($\bar{q}$). The three light-quark flavors (up, down and strange) suffice to explain the spectroscopy of most but not all of the charmless mesons lighter than the $\bar{c}c$ ground state (≈ 3 GeV/c^2).

Our understanding of how quarks form mesons has evolved within QCD, and we now expect a richer spectrum of mesons that takes into account not only the quark degrees of freedom but also the gluonic degrees of freedom. Gluonic mesons with no quarks (glueballs) are expected. Since the expected quantum numbers of low-lying glueballs (below 4 GeV/c^2) are not exotic, they should manifest themselves as extraneous states that cannot be accommodated within $q\bar{q}$ nonets [2]. Thus, their unambiguous identification is complicated by the fact that they can mix with $q\bar{q}$. Excitations of the gluonic field binding the quarks can also give rise to so-called hybrid mesons that can be viewed as bound states of a quark, antiquark and valence gluon ($q\bar{q}g$).

An alternative picture of hybrid mesons, supported by lattice QCD [3], is one in which a gluonic flux tube forms between the quark and antiquark and the excita-

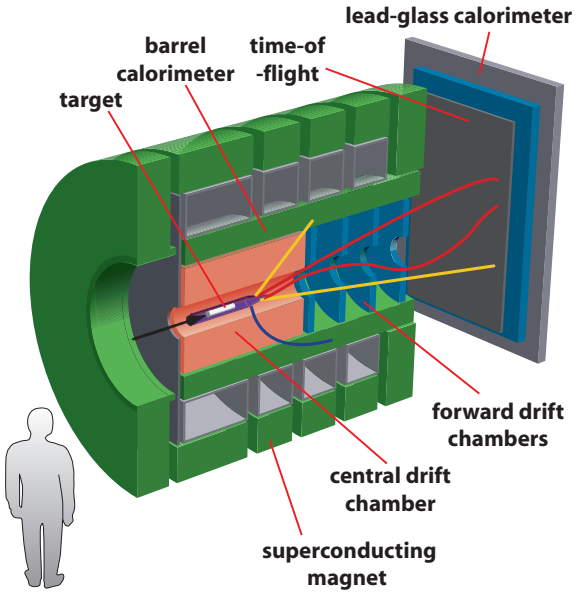

FIG. 1. A cut-away view of the GlueX detector. See Section VI for a description of the components.

* Spokesperson: Curtis A. Meyer, (cmeyer@cmu.edu)

tions of this flux tube lead to so-called hybrid mesons. Conventional $q\bar{q}$ mesons arise when the flux tube is in its ground state, while hybrid mesons arise when the flux tube is excited. In many models, some hybrid mesons can have a unique signature, exotic (not allowed for in a simple $q\bar{q}$ system) J^{PC}s. This signature simplifies the spectroscopy of these exotic hybrid mesons because they do not mix with conventional $q\bar{q}$ states. Lattice calculations presented in Section III support the existence of exotic-quantum-number states within the meson spectrum, independent of specific models.

The GlueX detector (shown in Figure 1) has been designed to observe these exotic-quantum-number hybrid states . A program in spectroscopy, supported by a sophisticated amplitude analysis, will map out the spectrum of the exotic-quantum-number states. At the same time, the spectrum of the normal $\bar{q}q$ mesons will be studied. Detailed comparisons of our experimental results to theoretical predictions on the excitations of the gluonic field in mesonic systems will lead to a more detailed understanding of the role of glue in the confinement of quarks inside hadronic matter.

II. MESON SPECTROSCOPY AND THE SEARCH FOR QCD EXOTICS

Despite an active experimental program, data supporting the existence of these states are still sparse. Recent review articles [2, 4, 5] provide a summary of the field. Briefly, evidence exists for up to three isovector, $J^{PC} = 1^{-+}$, exotic-quantum-number states: $\pi_1(1400)$, $\pi_1(1600)$ and $\pi_1(2015)$ (whose properties are summarized in Table I). The lightest state, the $\pi_1(1400)$, may not be a resonance. If it is resonant, it is almost certainly not a hybrid meson, rather, it is more naturally explained as a four-quark object [6].

The $\pi_1(1600)$ and the $\pi_1(2015)$ are both potential candidates for hybrid mesons. The $\pi_1(1600)$ suffers from a number of inconsistencies in its production, which appears different depending on how the π_1 decays. There is also a good deal of controversy about its $\rho\pi$ decay, with the existence of the decay mode apparently strongly dependent on assumptions in the analysis. However, the number and variety of the experimental results suggest that this state does exists. The highest-mass state is the result of very-low statistics analysis from a single experiment (E852), and needs confirmation. Either of these higher-mass states are consistent with lattice predictions for the mass of the π_1 hybrid. If both of these states are confirmed, they could be explained as the ground and first-excited states of the 1^{-+} system. A result which appears consistent with recent lattice calculations discussed below.

As noted above, the $\rho\pi$ (3π) decay mode of the $\pi_1(1600)$ remains controversial. In 2005, a high-statistics analysis of E852 data showed that the signal for the $\pi_1(1600)$ could be attributed to feed-through from the well-established $\pi_2(1670)$ due to the use of an incomplete set of the known π_2 decays in the analysis [7]. The VES experiment observed the $\pi_1(1600)$ in its other three observed decay modes, but they were never able to confirm the 3π decay of the $\pi_1(1600)$ (even with large statistics) [9]. Recently, the COMPASS experiment at CERN published their first results on 3π final states produced in peripheral pion production on nuclear targets [10, 11]. They report a robust signal for the $\pi_1(1600)$ in 3π, which is shown in Figure 2. Their analysis appears to include all the decays of the $\pi_2(1670)$, but the published information is still limited and their results are somewhat surprising in that both the $\pi_2(1670)$ and the $\pi_1(1600)$ have virtually the same mass and width. This is most clearly seen by the lack of phase motion between these two states, shown in Figure 2, and leads to concerns that the exotic state may be the result of unaccounted for feed-through from the stronger π_2 state, possibly caused by the use of the isobar model. Additional studies looking at other final states of the $\pi_1(1600)$ will be required if this issue is to be resolved.

In photoproduction, the CLAS collaboration has carried out the first search for the $\pi_1(1600)$ using a $4-5$ GeV photon beam and looking in the 3π final state. They see no evidence for the $\pi_1(1600)$ in their analysis [12]. This result could indicate that the $\pi_1(1600)$ does not decay to 3π, it is not produced in photoproduction, or both. In summary, while the $\pi_1(1600)$ appears reasonably solid via its other decay modes ($\eta'\pi$, $b_1\pi$ and $f_1\pi$), the simple 3π mode has been called into question and needs clarification.

While there is evidence for the isovector member of the $J^{PC} = 1^{-+}$ nonet, we also expect two isoscalar states (η_1 and η_1'), as well as two additional exotic nonets with $J^{PC} = 0^{+-}$ and 2^{+-}. There is still no experimental evidence for any of these other states. The former are necessary to establish the nonet nature of the π_1 states,

State	Mass (GeV)	Width (GeV)
$\pi_1(1400)$	1.351 ± 0.03	0.313 ± 0.040
$\pi_1(1600)$	1.662 ± 0.015	0.234 ± 0.050
$\pi_1(2015)$	2.01 ± 0.03	0.28 ± 0.05
State	Production	Decays
$\pi_1(1400)$	$\pi^- p$,$\bar{p}n$	$\pi^-\eta^\ddagger$,$\pi^0\eta^\ddagger$
$\pi_1(1600)$	$\pi^- p$,$\bar{p}p$	$\eta'\pi$,$b_1\pi$,$f_1\pi$,$\rho\pi^\ddagger$
$\pi_1(2015)$	$\pi^- p$	$b_1\pi$,$f_1\pi$
State	Experiments	
$\pi_1(1400)$	E852, CBAR	
$\pi_1(1600)$	E852, VES, COMPASS, CBAR	
$\pi_1(2015)$	E852	

TABLE I. The three exotic-quantum-number states for which some experimental evidence exists. The masses and widths are the Particle Data Group average [8]. The decays with a superscript ‡ are considered controversial.

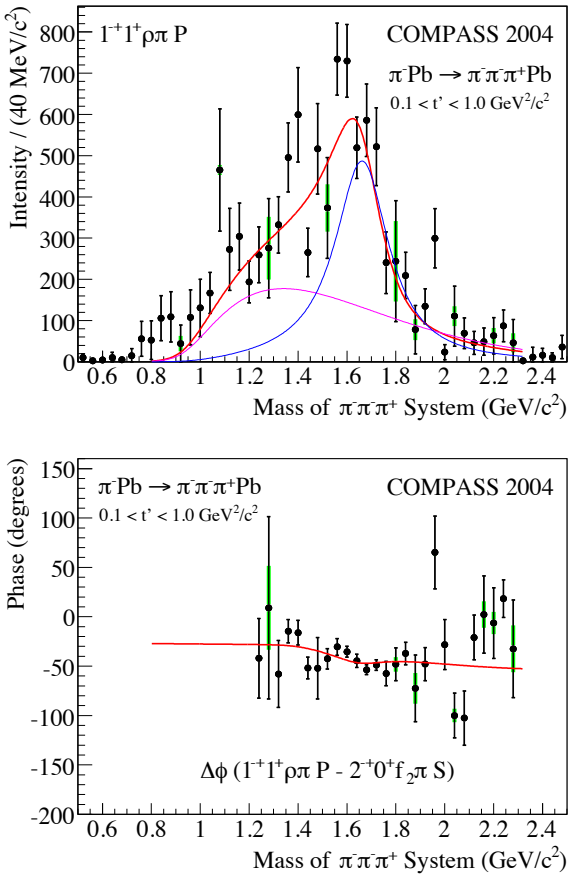

FIG. 2. The upper plot shows the intensity of the spin-exotic 1^{-+} $\rho\pi$ partial wave. The red curve shows the result of a mass-dependent fit with one Breit-Wigner for the $\pi_1(1600)$ (blue curve) on top of an unexplained background (purple curve). The lower curve shows the phase difference between the 1^{-+} ($\pi_1(1600)$) and the 2^{-+} ($\pi_2(1670)$) partial waves. Figure is taken from reference [11].

and the latter are expected in most models of hybrids. Table II lists the nine expected exotic-quantum number states as well as model predictions for their widths and decay modes. Mapping out the missing states remains a crucial activity.

Over the next several years, we anticipate that COMPASS will have new results based on a large data set recently collected on a proton target. These will be interesting extensions to higher beam energies of the diffractive pion production data collected by E852 and VES. COMPASS will also study central production, a program aimed at extending the work of the CERN WA102 experiment on the search for glueballs. COMPASS may be able to resolve the inconsistencies surrounding the $\pi_1(1600)$ in an unambiguous fashion in addition to confirming the existence of the $\pi_1(2015)$. They may also find other states. However, the COMPASS production mechanism is still limited to that studied in earlier experiments (E852 and VES) and may not provide a complete picture of the hybrid spectrum.

Name	$\mathbf{J^{PC}}$	Total Width (MeV)		Large Decays
		PSS	IKP	
π_1	1^{-+}	$81-168$	117	$b_1\pi$, $\rho\pi$, $f_1\pi$, $a_1\eta$
η_1	1^{-+}	$59-158$	107	$a_1\pi$, $f_1\eta$, $\pi(1300)\pi$
η_1'	1^{-+}	$95-216$	172	K_1^mK, K_1^lK, K^*K
b_0	0^{+-}	$247-429$	665	$\pi(1300)\pi$, $h_1\pi$
h_0	0^{+-}	$59-262$	94	$b_1\pi$, $h_1\eta$, $K(1460)K$
h_0'	0^{+-}	$259-490$	426	$K(1460)K$, K_1^lK, $h_1\eta$
b_2	2^{+-}	$5-11$	248	$a_2\pi$, $a_1\pi$, $h_1\pi$
h_2	2^{+-}	$4-12$	166	$b_1\pi$, $\rho\pi$
h_2'	2^{+-}	$5-18$	79	K_1^mK, K_1^lK, K_2^*K

TABLE II. Exotic quantum number hybrid width and decay predictions from reference [13]. The column labeled PSS (Page, Swanson and Szczepaniak) is from their model, while the IKP (Isgur, Karl and Paton) is their calculation of the model in reference [14]. The variations in width for PSS come from different choices for the masses of the hybrids. The K_1^l represents the $K_1(1270)$ while the K_1^m represents the $K_1(1400)$.

In addition to COMPASS, BES-III in Beijing has now been running for two years collecting data on the lightest charmonium states. Spectroscopy in the charmonium sector has undergone an extraordinary transformation in the last five years with the discovery over a dozen new states by the B-factory and Tevatron experiments. While none of the observed states exhibit exotic quantum numbers, several exhibit rather unusual properties in comparison to ordinary $c\bar{c}$ mesons. Space does not permit a comprehensive review here (see for example reference [15]). Definitive conclusions on the nature of these states, whether four-quark, hybrid, or simply excited charmonia, will need additional analysis and/or dedicated running by future experiments such as the p$\bar{p}$ annihilation experiment PANDA (at GSI), which will begin taking data in the charmonium region after the start of GlueX.

Decays of charmonium also provide an opportunity for studying and searching for light-quark exotic states. The BES III experiment in Beijing has been collecting e^+e^- data in the 3-4 GeV region for the past two years and currently has over 10^8 J/ψ and ψ' decays on disk. Many of the lightest charmonium bound states decay via $c\bar{c}$ annihilation into light hadrons. An amplitude analysis can then used to extract the properties of the intermediate resonances. While several potential exotic production channels have been identified, *e.g.,* $\chi_{c1} \rightarrow \pi_1\pi$, rates are uncertain. While GlueX remains unique in both its data set size and optimization for exotic production, it

is likely that BES III will provide complementary information on at least the spectrum of conventional mesons in the light quark sector in the next few years.

A thorough understanding of the spectrum of mesons in QCD demands these complementary efforts. With incredible statistics at modern experiments, a fascinating and puzzling spectrum has emerged in charmonium. This clearly needs further study. In addition we will want to understand if and how states like these emerge in the light quark sector and search for their exotic counterparts – GlueX will play a lead role in this search.

III. MESON SPECTROSCOPY AND LATTICE QCD

During the last five years, there have been several theoretical advances in our understanding of hybrid mesons. Most significant has been recent lattice QCD (LQCD) work which predicts the entire spectrum of light-quark mesons [16, 17]. The fully dynamical (unquenched) calculation is carried out with two flavors of light quarks and a heavier one tuned to the strange quark mass on two lattice volumes and four masses for the light quarks. These correspond to pion masses of 700, 520, 440 and 390 MeV, where the heaviest case has the three quark masses the same at the strange mass. For the heaviest case, the computed spectrum of isovector states is shown in Figure 3 (where the mass is plotted as a ratio to the Ω-baryon mass (1.672 GeV)). In the plot, the right-most columns correspond to the exotic π_1, b_0 and b_2 states. Interestingly, the 1^{-+} π_1 is the lightest, and that both a ground state and what appears to be an excited state are predicted. The other two exotic-quantum number states appear to be somewhat heavier than the π_1 with an excited state for the b_2 visible.

In addition to performing the calculation near the physical quark mass, there are a number of important innovations. First, the authors have found that the reduced rotational symmetry of a cubic lattice can be overcome on sufficiently fine lattices. They used meson operators of definite continuum spin *subduced* into the irreducible representations of cubic rotations and observed very strong correlation between operators and the spin of the state. In this way they were able to make spin assignments from a single lattice spacing. Second, the unprecedented size of the operator basis used in a variational calculation allowed the extraction of a great many excited states with confidence.

There were also phenomenological consequences of these lattice results. A subset of the meson operators used feature the commutator of two gauge-covariant derivatives, equal to the field-strength tensor which is non-zero only for non-trivial gluonic field configurations. Large overlap onto such operators was used to determine the degree to which gluonic excitations are important in the state, *i.e.*, what we would call the *hybrid* nature of the state. In particular, the exotic quantum number states all have large overlap with this type of operator, a likely indication hybrid nature over, say, multiquark structure.

In order to be able to extract the masses of states to be comparable with experiment, it is necessary to work at the physical pion mass. While work is currently underway to extract a point at $m_\pi \approx 280$ MeV, this limit has not yet been reached. To attempt to extrapolate, one can plot the extracted state masses as a function of the pion mass squared, which acts as a proxy for the light quark mass (see Figure 4). While linearly extrapolating to the physical pion mass ignores too much expected physics, it is probably safe to say that both the $\pi_1(1600)$ and the $\pi_1(2015)$ could be consistent with the expected 1^{-+} mass. They are also consistent with the ground and first-excited π_1 state. It appears that the b_0 and b_2 masses will likely be several hundred MeV heavier than the lightest π_1. These masses are all within the designed mass reach of GlueX.

Perhaps the most striking element of this calculation is the strong correlation with quark model predictions for the normal $q\bar{q}$ states [18], but only if they are supplemented with *non-exotic* hybrid meson states. The flux-tube model is an example of a framework which includes both the conventional and hybrid states in a seamless way. In the non-exotic $J^{PC} = 1^{--}$ sector, the lattice calculations extract six states (shown as red boxes in Figure 3) near 0.7, 1.1, 1.2, 1.3, 1.55 and 1.6 m_Ω. The quark model predicts five conventional states in this mass region, 1^3S_1, 1^3S_1, 1^3D_1, 3^3S_1 and 2^3D_1. In examining the operator content of the lattice states, the state near 1.3 has a large overlap with operators requiring a non-trivial gluonic field component, while the other states mostly do not. We also note that the state at 1.3 roughly lines up in mass with the exotic quantum numbered states. This is compatible with the picture suggested by the flux-tube model amongst others, namely degenerate exotic and non-exotic hybrid mesons. Similarly, in the $J^{PC} = 2^{-+}$ sector (π_2), the quark model predicts two states, the 1^1D_2 and the 2^1D_2 while the excited flux-tube model adds a non-exotic hybrid state. The lattice calculations indeed show three states, at 1.2, 1.4 and 1.6 m_Ω, with the middle one having a large overlap with the non-trivial gluonic-field operators. There also appears to be a hybrid pseudoscalar and possibly positive parity non-exotic hybrid states.

These recent lattice calculations are extremely promising. They reaffirm that hybrid mesons form part of the low-energy QCD spectrum and that exotic quantum number states exist. They also provide, for the first time, the possibility of assessing the gluonic content of a calculated lattice state. Similar calculations are currently underway for the isoscalar sector where preliminary results [19] for the mass scale appear consistent with those shown here in the isovector sector. These calculations will also extract the flavor mixing angle, an important quantity for phenomenology.

There are also new theoretical calculations relevant to the photo production of hybrid mesons. Lattice cal-

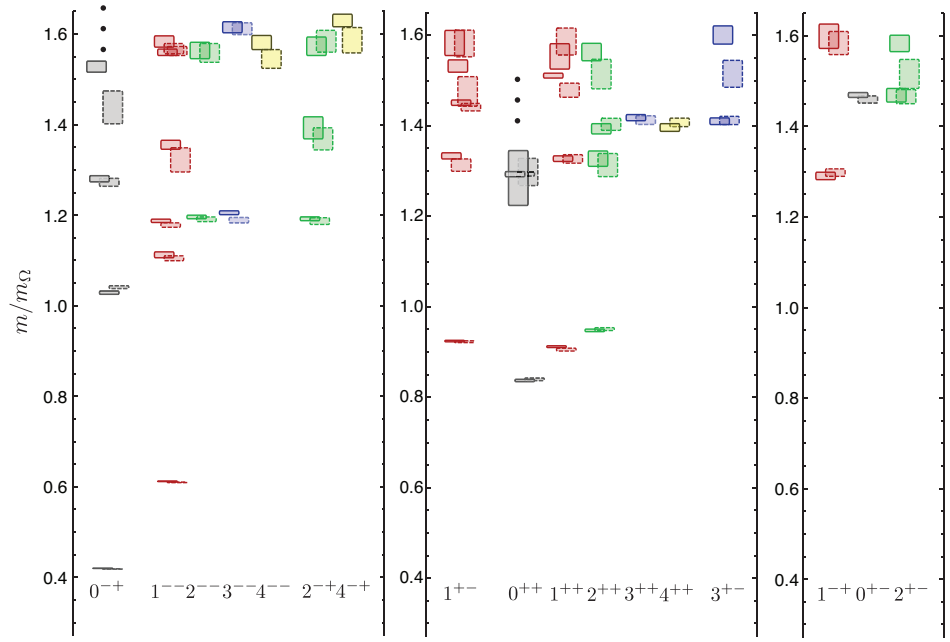

FIG. 3. The LQCD prediction for the spectrum of isovector mesons. The quantum numbers are listed across the bottom, while the color denotes the spin. Solid (dashed) bordered boxes on a $2.0^3(2.4^3)$ fm volume lattice, little volume dependence is observed. The three columns at the far right are exotic-quantum numbers. The plot is taken from reference [17] .

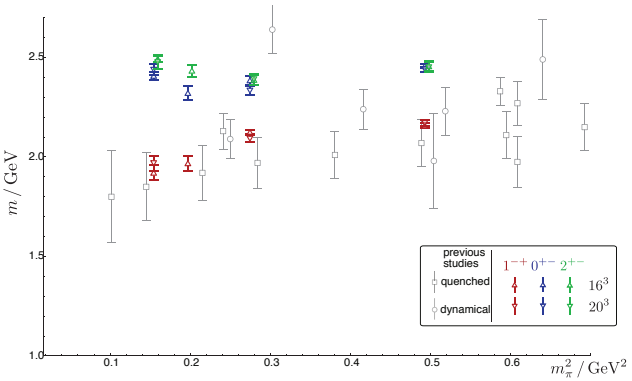

FIG. 4. The mass of the isovector exotic states as a function of m_π^2 used as a proxy for the light quark mass. Data are taken from reference [17].

culations in the charmonium sector looked at radiative decays of $c\bar{c}$ states [20, 21]. Rates were computed for a number of decays of conventional $c\bar{c}$ states, and found to be in quite reasonable agreement with experiment, thus yielding confidence in the calculation and the procedure of extracting rates. Based on this, the radiative decay of the 1^{-+} hybrid charmonium state (η_{c1}) to $J/\psi\,\gamma$ was computed. The rate was found to be large on the scale of conventional decays, and to proceed dominantly through an magnetic-dipole ($M1$) transition. This transition involves a spin-flip for normal $c\bar{c}$ states and is typically suppressed by the heavy charm-quark mass. In the hybrid system, no spin-flip appears to be needed as the gluonic field provides the one unit of angular momentum within a quark spin-triplet hybrid. Work is underway to extend these calculations to the light-quark sector where they will be directly applicable to GlueX. However, the charmonium results tend to support the suggestion of the flux-tube model [22, 23], that hybrid meson photoproduction is at least as large as that of normal $q\bar{q}$ states.

IV. GLUEX DATA ANALYSIS

Since our original PAC-30 presentation, we have developed hit-level detector simulation, reconstruction, and analysis software package to replace the parametric Monte Carlo that was used in the initial detector design. A full GEANT model of Hall-D/GlueX (HDGEANT) starting from the bremsstrahlung target and continuing through the GlueX detector exists and has been used extensively to model background rates in the detector as well as study physics reactions in GlueX. The Monte Carlo can be fed with a number of event generators, including a tuned version of the PYTHIA [24] that can simulate the entire photo-hadron cross section and is used to produce background event samples. The events from

HDGEANT can be fully reconstructed and used to study physics processes, optimize detector design, and understand the impact of changes to the detector system. The running of our simulation has taken advantage of work done by our collaboration to implement Open Science Grid (OSG) software for GlueX. Currently we are able to run Monte Carlo simulation for GlueX on the OSG and our data is cached and retrieved from grid storage using OSG tools. We are continuing to enhance our reconstruction framework in a number of ways, e.g., optimizing speed of algorithms, developing Kalman filtering to improve our estimates of errors, suppressing secondary hadronic showers in calorimeter, *etc.*...

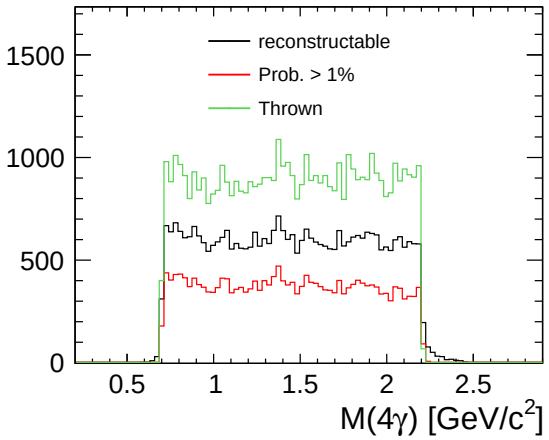

FIG. 5. The $\gamma\gamma\gamma\gamma$ invariant mass from reference [25]. The green curve represents the generated events, the black curve are those that are reconstructable (about 65 to 70%), while the red curve are those events which satisfy a six-contraint kinematic fit at the 1% confidence level (about 50%).

Using these tools, a full analysis of the reaction $\gamma p \to \eta\pi^0 p$ (as part of the first Ph.D. thesis on GlueX [25]) has been carried out. This analysis mixed a Monte Carlo $\eta\pi^0 p$ event sample with a full sample of PYTHIA background events. The events were then passed through the HDGEANT simulation and reconstructed using the GlueX/Hall-D analysis code. The resulting events were then further processed using kinematic fitting combined with various kinematic cuts to separate signal from background. While not fully optimized, the acceptance for a final state with four photons and a proton is around 50%. This is shown in Figure 5 where the curves represent the thrown sample, the reconstructable sample, and the sample after kinematic fitting to the $\eta\pi^0 p$ final state. This analysis also obtains a signal to background ratio for the $\eta\pi^0$ events on top of the PYTHIA background that is typically between two and five. The ability to carry out analyses such as this one allow us to focus work on improving our reconstruction algorithms .

In summary, our simulation and analysis software is now capable of performing full physics analyses.We have also used it to optimize the design of the detector and, as will be seen in the following section, to develop our amplitude analysis code. We have successfully used the OSG for generating Monte Carlo events and are currently exploring the for storage and retrieval of data sets. Finally, a standard event sample ($b_1\pi$) events is now automatically run through the analysis chain on regular basis to monitor the stability of the code and flag problems as development continues.

V. GLUEX AMPLITUDE ANALYSIS

The discovery of exotic-quantum-number mesons in the photo-production data from GlueX hinges on an amplitude analysis to extract the signals. These analyses will take as input measured four-vectors of both reconstructed and simulated events. An unbinned maximum likelihood fit is then used to determine the physics model which makes the real and simulated event distributions agree. The physics model includes both known processes, possible new mesons, and backgrounds, with the crucial extracted signal being intensities and phase differences. If these are robust over several related final states, it is then possible to extract masses and widths of mesons from the data.

A multi-faceted approach is being utilized for the development of analysis tools for GlueX, with a significant portion of the effort funded by an NSF Physics at the Information Frontier grant awarded to a subset of GlueX collaborating institutions. The ability to capitalize on the high-statistics, high-quality data that GlueX will provide depends on two developments. First, work needs to be done on the phenomenology so that theoretical assumptions inherent in the analysis, *e.g.*, the isobar model, can be reduced or quantified. Second, fitting and computational technology to handle both the large volumes of data and computationally-intensive phenomenological models needs to be developed. Both of these challenges are being tackled now with both simulated GlueX data and data from existing experiments.

An example analysis comes from a recent work on the photo production of ω mesons in CLAS [26]. This was carried out by GlueX collaborators who are also members of CLAS using analysis tools that were developed to be useful for GlueX [27]. Figure 6 shows the strength of the dominant waves in the data (upper) and the phase difference between two s-channel contributions (lower). The phase difference requires two nearby $J^P = (\frac{5}{2})^+$ resonances to describe it. The lower is the four-star $F_{15}(1680)$ while the higher-mass state is an $F_{15}(1950)$, a state that is considered one of the *missing baryons*. The interference with the $(\frac{7}{2})^-$ $G_{17}(2190)$ is crucial in extracting this result.

In an attempt to enhance the collaboration with theory colleagues, fitting software has been designed in a

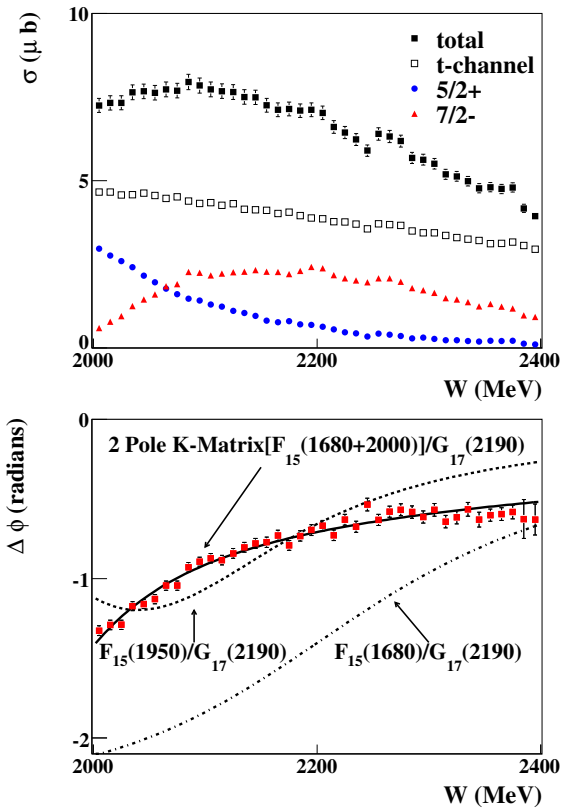

FIG. 6. Results from the amplitude analysis of $\gamma p \to \omega p$. The upper plot shows the intensity of the contributions to the total cross section, with the dominant signals being t-channel pion exchange, and $J^P = (\frac{5}{2})^+$ and $(\frac{7}{2})^-$ partial waves. The lower figure shows the phase difference between the two s-channel waves, which requires two interfering $(\frac{5}{2})^+$ resonances to describe the data. The plots are taken from reference [26].

modular way so that theoretical expressions for the decay amplitudes can easily be inserted and modified. In addition, the expression for the decay amplitude may have an arbitrary number of free parameters. Such flexibility requires the computational capability to recompute each parametrized decay amplitude for each event at every fit iteration, an option that, in the past, has been difficult due to limited computing capability. Our proposed solution to this problem involves parallalization of the amplitude computation, which can be done independently for each event, at several levels. At the level of the main fitting process, the software utilizes Message Passing Interface (MPI) to allow many processes on multiple cores or multiple nodes in a cluster to work cooperatively in fitting a single data set. This provides, modulo overhead, a $1/N_p$ scaling of the fit time, where N_p is the number of processes.

Beyond this simple per-processor parallalization, it is now possible to dramatically accelerate the fitting process utilizing the massive hardware parallalization and computational capability of graphics processing units (GPUs). In order to explore this new tool, we have ported event-by-event amplitude calculation to GPUs. Even without significant optimization, this simple change yielded a speed gain of one to two *orders of magnitude* utilizing year-old hardware. The newest hardware doubles the number of computational cores (to 400) and significantly enhances memory access and double precision computation. Our initial work with GPUs has dramatically changed the way that we now view amplitude analysis in GlueX. We now expect that a multi-process solution, with each process utilizing a single GPU, can meet the initial demands GlueX amplitude analysis with current hardware. While it is difficult to anticipate the state-of-the-art at the time GlueX comes on line, we believe that we have the technology now to do the initial GlueX amplitude analyses.

These software developments have been prototyped on actual data analysis within the context of the CLEO-c and CLAS experiments. In the CLEO-c case, careful software optimization as well as migration to GPUs has reduced time to fit modest data samples from tens of minutes to several seconds. This work is providing a prototype interaction with theory colleagues, who are contributing to the development of the amplitudes to describe the data. In the case of CLAS, software tools have been developed to aid in error-free coding of complicated quantum mechanical amplitudes (initially for excited baryons). The CLAS work on ω photoproduction discussed above has provided an opportunity to understand how to deal with backgrounds in high-dimensional analyses [28] as well as improving goodness-of-fit measures for likelihood fitting [29]. Combined with our enhanced GlueX simulation and analysis capability, discussed in the preceding section, these tools have set the stage for a full "data analysis challenge" that involves simulation of a key GlueX physics process and all of its backgrounds followed by full reconstruction, event selection, and amplitude analysis. Software is nearly complete, to generate, reconstruct, and fit simulated data for the reactions $\gamma p \to \pi^+\pi^+\pi^- n$, where we expect to search for the $\pi_1(1600)$, and $\gamma p \to b_1\pi p$, a model-favorite for hybrid decay. During the design stage of GlueX, such studies were performed using fast parametric Monte Carlo to check and validate the experimental design. Repeating them now, with a full detector simulation including backgrounds, is an investment in software infrastructure and analysis expertise that can be utilized when GlueX comes on line. We anticipate the first detailed "analysis challenges" for GlueX to be complete by the end of the year.

VI. UPDATES TO THE GLUEX EQUIPMENT

Figure 1 shows a cut-away view of the GlueX detector. Not shown is the tagger hall where the 9 GeV linearly-polarized photon beam is produced via the coherent bremsstrahlung process in a thin ($20\,\mu m$) diamond crystal. The scattered electron from the bremsstrahlung process is detected in a tagger array instrumented with a very fine scintillators (the microscope) at the coherent peak, and a coarser-grained set of counters spanning most of the remaining energy range. After travelling 80 meters, the photon beam is scraped using a 3 mm diameter collimator and passes through a pair spectrometer for monitoring flux, energy and polarization.

The photons then interact in a liquid-hydrogen target and the resulting charged particles and photons are detected in GlueX. Charged particles travel through a scintillator-based start counter which is just outside the target volume. They are then tracked through the 2.2 T solenoidal field in the central drift chamber (CDC) and the forward drift chamber (FDC) packages. Time-of-flight is measured in the forward TOF system as well as in the barrel calorimeter (BCAL). Inside the magnet bore, photons are detected in the BCAL (a lead-scintillating fiber calorimeter) and the signals are read out using field-insensitive silicon photomultipliers (SiPMs). In the forward direction, photons are detected in a lead-glass calorimeter (FCAL) which is downstream of the TOF.

During the last four years, the GlueX experiment and Hall-D have gone through extensive reviews as part of the Department of Energy's *Critical Decision* process. These external reviews focused on all aspects of the detector, and the reviewers not only vetted the design of the experiment, but also made suggestions to improve GlueX and reduce the cost and risk of the project. Because of the closely coupled nature of both GlueX and Hall-D, the collaboration has been a very active participant in all of these reviews, a list of which can be found in Table III. As a result of this extensive review process, there have been a number of changes to the GlueX detector that are discussed below.

Review	Date
Drift chamber review	March 2007
FDC technology review	February 2008
Calorimeter design review	February 2008
Tracking and PID final design review	March 2008
System and infrastructure design review	May 2008
IPR Lehmann review	July 2008
Beamline and tagger review	November 2008
Installation review	February 2009
Tagger magnet design review	July 2009
BCAL readout review	July 2009
Solenoid magnet internal review	Nov 2009

TABLE III. A list of the GlueX/Hall-D externals reviews which were part of the DOE decision process.

Contract	Group	Status
Tagger	UCONN	in process
Tagger	CUA	in process
Tagger	NCA& T	in process
Pair Spect.	UNC Wilmington	in process
Target	UMASS	in process
Start Counter	FIU	in process
CDC	CMU	in place
FDC	JLab	in place
FDC	UVA	in discussion
BCAL	U. Regina	in place
BCAL Readout	Santa Maria	in process
TOF	FSU	in process
FCAL	I.U.	in place
Solenoid	JLab	in place
Solenoid	IUCO	in place
Trigger	CNU	in process
Electronics	JLab	in place
Electronics	UMASS	in process

TABLE IV. The construction contracts for GlueX.

The most significant change to the GlueX detector has been the descoping of the Cerenkov system for particle identification. This was done by the 12-GeV project to increase contingency funds for the rest of the project. The collaboration is actively seeking new groups who would be interested in designing and building this system using funds outside of the 12-GeV project, either from NSF MRI funds, or as part of a post-CD4 detector improvement.

Improvements and changes have also been made to many of the detector systems in Hall-D and GlueX. In the tagger system, the original two-magnet design has been replaced by a single magnet which reduces cost and improves alignment issues. Improvements in the primary beam have allowed us to reduce the transverse dimension of the diamond radiator from 8 mm to 4 mm. The maximum tagged photon energy has been increased from 11.4 GeV to 11.7 GeV. For photons above 9 GeV, 100% of the photons are now tagged (up from 50%). These changes will allow for other experiemnts to better take advantage of the highest energy photons in Hall-D. Modifications have also been made to the primary and secondary photon-beam collimators that will make it easier to change size of the collimator hole. Lastly, we now have a full design for the pair spectrometer system.

A major overhaul is being performed on the GlueX solenoid. This has been necessary to fix a number of leaks and shorts in the system. The iron yoke in the

solenoid has been redesigned to fill gaps in the earlier design. This improves the overall magnetic field shape, and reduces the amount of saturated magnetic material. First cold tests of the refurbished coils are scheduled for summer of 2010.

In order to improve the overall tracking efficiency and the resolution of the detector, the CDC has been shortened by about 10%, the fraction of stereo layers has been increased, and a tighter packing of the straws has led to an increase in the number of layers by four. To reduce material in the tracking volume, the down stream end plate is thinner and made of carbon fiber. The FDC has had significant material removed from the tracking volume, reducing the number of radiation lengths in each of the four FDC packages from 1.4% to 0.4%. Material has also been reduced in the frames, with the average thickness about 50% of the earlier design. A full-scale prototype of a module is currently being completed at Jefferson Lab and studies of this show that the design resolution has been exceeded by up to a factor of two.

For the TOF, we will be using a faster photomultiplier (10 stage Hamamatsu R10533) tubes to improve timing and a somewhat thicker scintillator to better match the photomultiplier size.

A final decision was made to readout the BCAL using SiPMs. These form a compact readout that is very close to the detector which eliminates light guides and is insensitive to the magnetic field. We have also found that the attenuation length of the scintillating fibers is exceeding specification by a large margin. These effects lead to the number of collected photo electrons far exceeding the original specifications which leads to improved detector performance. In the FCAL, the designs for both optical coupling of the lead-glass blocks to the photomultipliers (PMTs) and the magnetic shielding for the PMTs has been finalized. By using a silicon-based optical joint as part of the light-coupling scheme, light collection efficiency has been enhanced by a factor of 2-3 over the earlier designs. In the new design, each glass block assembly will be built as a module rather than having a large array of PMTs, thus simplifying the design and assembly.

Construction has started on the BCAL, the FCAL and the CDC, and the first eight (of 48) BCAL modules have been delivered to Jefferson Lab. Construction on other elements will start over the next two years at institutions around the world. A summary of the construction contracts needed to build GlueX is shown in Table IV. Finally, based on the detailed prototype work carried out for GlueX, we have continued to publish instrumentation papers. From work on the BCAL, results of our beam test in Hall-B [30] as well as information on the spectral response of scintillating fibers [31] have been published. In addition, we have written an article on the CDC [32] and one on the analysis of signal pulses in the the FCAL [33].

VII. OTHER PHYSICS OPPORTUNITIES

The GlueX collaboration is actively seeking to enhance its physics program beyond meson spectroscopy. In March of 2008, the collaboration organized a workshop [34] at Jefferson Lab, "Photon-hadron physics with the GlueX detector at JLab" that was attended by about 70 people. A number of interesting ideas came out of this meeting and one has matured to an accepted proposal.

The PrimEx experiment at 12-GeV was approved by PAC-35 to run using the Hall-D beam line and the GlueX detector. The proponents of this proposal have joined GlueX and the collaboration as a whole worked on the final proposal that was submitted in December 2009.

A physics topic that is maturing within the collaboration is baryon spectroscopy, and in particular, the spectrum of double-strange Cascade baryons (Ξs). Only a few of these states are well established. Many more states must exist; if not, our understanding of baryon structure is fundamentally flawed. It would be interesting to see the lightest excited Ξ^* states in certain partial waves decoupling from the $\Xi\pi$ channel, a confirmation of the flavor independence of confinement. Measurements of the isospin splittings in spatially excited Ξ states are also needed. Currently, these splittings like $n-p$ or $\Delta^0-\Delta^{++}$ are available for the octet and decuplet ground states, but are hard to measure in excited N, Δ and Σ, Σ^* states, which are very broad. Many cascade baryons are likely to be narrow and measuring the $\Xi^- - \Xi^0$ splitting of spatially excited Ξ states remains a strong possibility. These measurements are an interesting probe of excited hadron structure and would provide important input for quark models that describe the isospin splittings by the u- and d-quark mass difference as well as by the electromagnetic interactions between the quarks.

Other interesting ideas such as inverse DVCS, threshold charm production, and photo-nuclear interactions have also been considered. We anticipate that future study of these topics in the context of GlueX will occur both within the collaboration and through the hosting additional physics workshops.

VIII. SUMMARY

The experimental search for exotic-quantum-number mesons continues to be an exciting problem, albeit one which is limited by the current data. These data support the picture of two isovector $J^{PC} = 1^{-+}$ states, the $\pi_1(1600)$ and the $\pi_1(2015)$. However, limited statistics mean that confirmation is needed, particularly for the higher-mass state. Recent progress in LQCD reaffirms the existence of exotic-quantum-number mesons, and their large overlap to *non-trivial* gluonic fields. It also predicts the existence of normal quantum number hybrids and provides a method of measuring the overlap with the gluonic fields, all of this independent of specific

models of QCD. Other LQCD calculations support the picture that photoproduction is indeed a good place to search for hybrid mesons. These calculations also suggest that two isovector $J^{PC} = 1^{-+}$ states are expected, but many unobserved states are also expected.

Over the next several years, we anticipate new results from the COMPASS experiment at CERN which will continue to explore the diffractive pion production studied by E852 and VES. An active program of spectroscopy both in the charmonium and light-quark sector is underway at BES III. The PANDA experiment at GSI is expected to start search for both glueballs and charmonium hybrids in $p\bar{p}$ annihilation on a time scale commensurate with first results from GlueX.

GlueX remains unique in its high-statistics exploration of photoproduction, a complementary environment to other experiments, that is expected to be rich in exotic mesons. In addition to detector construction, the collaboration is pursuing an aggressive effort in software and analysis development with the goal of being ready for physics analysis when first 12 GeV production beam is available.

[1] The GlueX Collaboration, "Mapping the Spectrum of Light Quark Mesons and Gluonic Excitations with Linearly Polarized Photons", GlueX-doc 1226, January (2006), (http://argus.phys.uregina.ca/cgi-bin/public/DocDB/ShowDocument?docid=1226).

[2] V. Crede and C. A. Meyer, Prog. Part. Nucl. Phys. **63**, 74 (2009).

[3] G. S. Bali *et al.* [TXL Collaboration and T(X)L Collaboration], Phys. Rev. D **62**, 054503 (2000).

[4] Eberhard Klempt and Alexander Zaitsev, Phys. Rep. **454**, 1, (2007).

[5] C. A. Meyer and Y. Van Haarlem, submitted to Phys. Rev. C, (2010), arXiv:1004.5516 [nucl-ex].

[6] S. U. Chung, E. Klempt and J. G. Korner, Eur. Phys. J. A **15**, 539 (2002).

[7] C. Amsler, *et al.* [The Particle Data Group], Phys. Lett. B**667**, 1, (2008).

[8] A. R. Dzierba *et al.*, Phys. Rev. D **73**, 072001 (2006).

[9] D. V. Amelin *et al.* [VES Collaboration], Phys. At. Nucl. **68**, 359, (2005).

[10] A. Alekseev *et al.* [The COMPASS Collaboration], Phys. Rev. Lett. **104**, 241803, (2010).

[11] B. Grube *et al.* [The COMPASS Collaboration], arXiv:1002.1272 [hep-ex] (2010).

[12] M.Nozar *et al.* [CLAS Collaboration], Phys. Rev. Lett. **102**, 102002, (2009).

[13] P. R. Page, E. S. Swanson and A. P. Szczepaniak, Phys. Rev. D **59**, 034016 (1999).

[14] N. Isgur, R. Kokoski and J. Paton, Phys Rev. Lett. **54**, 869, (1985).

[15] E. S. Swanson, Phys. Rept. **429**, 243 (2006).

[16] J. J. Dudek, R. G. Edwards, M. J. Peardon, D. G. Richards and C. E. Thomas, Phys. Rev. Lett. **103**, 262001 (2009).

[17] J. J. Dudek, R. G. Edwards, M. J. Peardon, D. G. Richards and C. E. Thomas, submitted to Phys. Rev. D, (2010), arXiv:1004.4930 [hep-ph].

[18] S. Godfrey and N. Isgur, Phys. Rev. D **32**, 189 (1985).

[19] J. J. Dudek, private communication.

[20] J. J. Dudek, R. G. Edwards and D. G. Richards, Phys. Rev. D **73**, 074507 (2006).

[21] J. J. Dudek, R. Edwards and C. E. Thomas, Phys. Rev. D **79**, 094504 (2009).

[22] F. E. Close and J. J. Dudek, Phys. Rev. Lett. **91**, 142001 (2003).

[23] F. E. Close and J. J. Dudek, Phys. Rev. D **69**, 034010 (2004).

[24] `http://home.thep.lu.se/ torbjorn/Pythia.html`.

[25] Blake D. Leverington, "The GlueX lead-scintillating fibre electromagnetic calorimeter", Ph.D. Thesis, University of Regina, (2010).

[26] M. Williams *et al.* [CLAS Collaboration], Phys. Rev. C **80**, 065209 (2009).

[27] M. Williams, Comp. Phys. Comm. **180**, 1847, (2009).

[28] M. Williams, M. Bellis, C. A. Meyer, JINST **4**, P10003, (2009).

[29] M. Williams, Submitted to JINST, (2010), arXiv:1006.3019 [hep-ex].

[30] B.D. Leverington *et al.*, Nucl. Instrum. Meth. A**596**, 327 (2008).

[31] Z. Papandreou, B.D. Leverington and G.J. Lolos, Nucl. Instrum. Meth. A**596**, 338 (2008).

[32] Y. Van Haarlem, C.A. Meyer, *et al.*, Accepted for publication in Nucl. Instrum. Meth. (2010), arXiv:1004.3796 [nucl-ex].

[33] J. Bennett, M. Kornicer, M. Shepherd *et al.*, Accepted for publication in Nucl. Instrum. Meth. (2010), arXiv:1005.5349 [physics.ins-det].

[34] http://www.jlab.org/Hall-D/meetings/php2008/program.html.